Stator Core Flux Density Analytical Determination in Slotless Machines

Nada Elloumi, Matteo Leandro, Jonas Kristiansen Nøland, *Member, IEEE*
and Alberto Tessarolo, *Senior, IEEE*

***Abstract*—Slotless machines equipped with surface-mounted permanent magnet (SPM) rotor are used in such applications where the torque ripple and the additional losses due to the slotting effect are critical. For this kind of machine it is possible to have an accurate analytical solution for the magnetic fields in every machine cross-section domain. This paper derives an analytical expression for the magnetic field distribution inside the stator core of an SPM slotless machine for general load conditions. Different rotor magnetization patterns are also considered for board evaluation of the flux density. All results are compared with finite element analysis showing satisfactory accordance.**

***Index Terms*—Analytical method, Laplace equation, magnetic field, magnetization pattern, slotless machine, stator core.**

I. Introduction

In conventional PM machines, windings are fixed to a slotted stator core and usually retained with non-conductive wedges. The presence of slots in the stator topology is known to produce several parasitic phenomena like cogging torque and additional eddy current losses. In some applications, like wind power generation [1] or gas compression [2], it is necessary to overcome such issues in order to achieve very high efficiency and negligible torque ripples. One possible solution is to use the slotless stator structure. This kind of stator is designed to get rid of the slotting effect by distributing the windings along the bore of an annular stator core which are usually retained through a resin cast encapsulation. As widely treated in the literature, the design of such a machine can be approached by means of Finite Element Analysis (FEA) simulation tools possibly interfaced with design optimization programs [1], [3]. This approach suffers from the drawback of being very time consuming. Alternatively, Thanks to the absence of teeth, the slotless SPM machine geometry enables a relatively easy analytical solution for the magnetic fields in the active parts. For that, several previous works have addressed the analytical modeling of slotless SPM machines adopting the resolution of differential equation in order to compute the magnetic field in the slotless SPM machine [4]–[8]. Most of the literature dedicated to the analytical modeling of this kind of machine has focused on the air-gap magnetic field evaluation to predict the machine performance such as the calculation of back EMF, torque and inductance [8], [9]. Another work such as in [7] has proposed a more general analytical expression of the vector potential and the magnetic field has been developed considering a multi-layer cylindrical system to predict the field in a wider range of the machines' sub-domains taking into account the effect of eddy current in the conductive areas. However, it is noticeable that among all the aforementioned analytical modeling techniques dealing with slotless machines, little or no attention is paid to the machine stator core. Indeed, the prediction of the magnetic field in the stator core is crucial to estimate core losses which could have critical effect on the machine performance.In [10] an analytical approach to compute a two dimensional magnetic field distribution the stator has been developed yet considering a soft magnetic composite material (SMC) stator core. Moreover, a further approach has focused on the magnetic field prediction inside the stator core, but limiting the scope of the treatment to the no-load operation and just considering radial magnetization in the rotor [11].

The aim of this work is to extend the investigation proposed in [11] to develop an analytical expression for the total magnetic field (due to both stator and rotor) in the stator core of SPM slotless machines with a generic magnetization pattern (parallel, radial, Halbach). The availability of an explicit analytical magnetic field computation formula may enable the instantaneous estimation of the iron core losses (using, for example, the Bertotti's formulation [12]–[15]). An analytical expression for the magnetic field (both radial and tangential components) in the iron core is possible through the solution of Poisson and Laplace differential equations in the machine domains of interest (stator core, air gap, magnets).

In this paper, the explicit formulation for the total magnetic field is derived for SPM slotless machines covering different possible magnetization patterns: parallel, radially segmented and halbach magnetization. The accuracy of the proposed magnetic field expressions is then successfully assessed by comparison against Finite Element Analysis (FEA) for different numbers of poles and magnetization patterns.

N. Elloumi and A. Tessarolo are with the Engineering and Architecture Department, University of Trieste, Trieste, Italy (email: nada.elloumi@phd.units.it).

N. Elloumi is also with the National Engineering School of Sfax, University of Sfax, Tunisia.

M. Leandro and J. K. Nøland are with the Department of Electric Power Engineering, Norwegian University of Science and Technology, Trondheim, Norway.

II. Problem Definition and Model Assumptions

The slotless structure allows a direct solution for the magnetic field distribution inside every machine domain solving the Laplace/Poisson differential equations [6]. The rotor magnetization patterns addressed in this work are shown in Fig.1, where the arrows represent the magnetization direction inside the magnet's region.

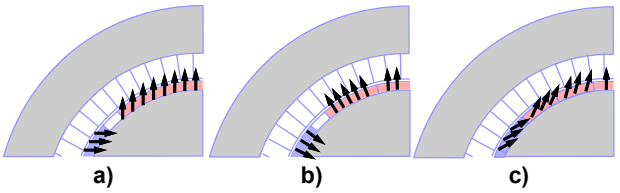

Fig. 1. Rotor types considered in the analysis. **a)** Parallel magnetization, **b)** radial segmented magnetization, **c)** halbach array magnetization.

The rotor types being covered are; 1) parallel magnetization Fig. 1a; 2) segmented radial magnetization Fig. 1b, where each pole is composed of N_{seg} parallel magnetized magnets blocks; 3) halbach magnetization pattern where each pole is composed of N_{seg} parallelly magnetized magnet blocks as well. These kinds of rotor magnetization patterns are commonly employed in permanent magnet machines [16], [17]. The field problem definition is based on the following simplifying hypothesis:

- Stator and rotor cores are assumed to have infinite magnetic permeability;
- The relative magnetic permeability of permanent magnets is considered to be equal to unity;
- End effects are disregarded; hence the vector potential is everywhere parallel to the rotational axis so that its axial component is always considered as a scalar quantity.
- The stator windings are assumed to carry a three phased balanced sinusoidal current.

III. Magnetic Field Evaluation in the Slotless Machine Stator Core

In this section, the total magnetic field distribution in the stator core is evaluated by superimposing the contributions of both stator windings and rotor magnets fields.

A. Computation of the Flux Density in the Stator Core due to Stator Currents

In order to evaluate the stator currents contribution in the total magnetic field, it has been necessary to solve the Laplace equation (1) in the domain named as "Stator region" as shown in Fig. 2. This region is bounded with two circumferences whose radii are R_2 and R_3 for the inner and outer bound respectively. In a cylindrical coordinate system (r,ϑ,z) centered in the machine rotational axis, the vector potential $\mathbf{A}$ in the stator region is governed by the Laplace differential equation as follows:

$$\nabla^2 \mathbf{A} = \frac{1}{r}\frac{\partial}{\partial r}\left[r\frac{\partial A_z}{\partial r}\right] + \frac{1}{r^2}\frac{\partial^2 A_z}{\partial \theta^2} = 0 \tag{1}$$

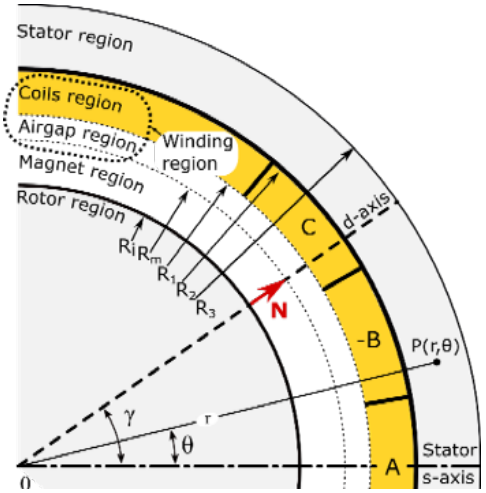

Fig. 2. Characteristic dimensions of the machine cross-section. Stator s-axis and rotor d¬axis are also represented.

where A_z is the scalar component of the vector potential.

Using the Fourier expansion taking into account the harmonics introduced by the field source, a solution of this kind of differential equation can be formulated as follows:

$$\begin{aligned} A_z(r,\theta,t) = &\sum_{k_p=5p,11p,\ldots}^{\infty} \left(V_{k_p}^{+} r^{k_p} + V_{k_p}^{-} r^{-k_p}\right)\cos(k_p\theta + \omega t) \\ &+ \sum_{k_m=1p,7p,\ldots}^{\infty} \left(V_{k_m}^{+} r^{k_m} + V_{k_m}^{-} r^{-k_m}\right)\cos(k_m\theta - \omega t) \end{aligned} \tag{2}$$

Where V_n^+ and V_n^- are constants that have to be determined defined for k_p and k_m. Thanks to the relationship between the magnetic vector potential and the flux density in a planar domain, the flux density produced by the coil currents in the stator region can be obtained as:

$$B_r^{st}(r,\theta) = \frac{1}{r}\frac{\partial A_z(r,\theta)}{\partial \theta} \tag{3}$$

$$B_\theta^{st}(r,\theta) = -\frac{\partial A_z(r,\theta)}{\partial r} \tag{4}$$

Using the latter equations, it is possible to determine the constants V_n^+ and V_n^- by imposing the following boundary conditions:

$$B_r^{st}(R_3,\theta) = \frac{1}{r}\frac{\partial A_z(R_3,\theta)}{\partial \theta} = 0, \tag{5}$$

along Γ_4 in Fig. 3.

$$B_r^{st}(R_2,\theta) = \frac{1}{r}\frac{\partial A_z(R_2,\theta)}{\partial \theta} = BS_r^{b.c.}(\theta,t), \tag{6}$$

along Γ_3 in Fig. 3.

The boundary condition (5) is due to the fact of imposing the homogeneous Dirichlet condition along the outer machine border. The second boundary condition (6) represents the radial magnetic field continuity between the winding region

and the stator region. As a consequence, $BS_r^{b.c.}(\theta,t)$ can be expressed using the results obtained in [6] as follows:

$$BS_r^{b.c.}(\theta,t) = -\sum_{k_p} \frac{k_p}{r} w(r,k_p)\sin(k_p\theta+\omega t) - \sum_{k_m} \frac{k_m}{r} w(r,k_m)\sin(k_p\theta-\omega t) \tag{7}$$

Where the function $w(r,n)$ is the part that accounts for the dependency on r and can be expressed for a generic n as follows :

$$w(r,n) = \begin{cases} W_n^+ r^n + W_n^- r^{-n} - W_n^* r^2, & \text{if } n \neq 2 \\ \dfrac{\mu_0 J_2}{4}\left[\dfrac{A+B(r)r^4}{4r^2(R_i^4-R_2^4)} - r^2\ln r\right], & \text{if } n = 2 \end{cases} \tag{8}$$

where coefficients A and $B(r)$ are given as:

$$A = R_1^4 R_2^4 - R_2^4 R_i^4 + 4R_2^4 R_i^4 \ln\left(\frac{R_1}{R_2}\right)$$
$$B(r) = R_1^4 - 2R_2^4 + R_i^4 + 4R_i^4 \ln\left(\frac{R_1}{r}\right) + 4R_2^4 \ln\left(\frac{r}{R_2}\right) \tag{9}$$

and coefficients J_n,W_n^+,W_n^- and W_n^* can be found in [6] in formulas (4), (15), (16) and (17).

The two coefficients V_n^+ and V_n^- of the Laplace equation solution are determined solving the set of two equations obtained by substituting (2) in (5) and (6). The solution of the the linear system yields:

$$V_n^- = \frac{R_2^n R_3^{2n}\cdot w(R_2,n)}{R_2^{2n}-R_3^{2n}} \tag{10}$$

$$V_n^+ = \frac{R_2^n \cdot w(R_2,n)}{R_3^{2n}-R_2^{2n}} \tag{11}$$

with the latter expressions being determined, the radial and tangential components of the magnetic field due to the stator currents are expressed as follows:

$$B_r^{st}(\theta,r,t) = -\sum_{k_p=5p,11p,\ldots}^{\infty} k_p\left(V_n^+ r^{k_p-1} + V_n^- r^{-k_p-1}\right)\sin(k_p\theta+\omega t) - \sum_{k_m=1p,7p,\ldots}^{\infty} k_m\left(V_n^+ r^{k_m-1} + V_n^- r^{-k_m-1}\right)\sin(k_m\theta-\omega t) \tag{12}$$

$$B_\theta^{st}(\theta,r,t) = -\sum_{k_p=5p,11p,\ldots}^{\infty} k_p\left(V_n^+ r^{k_p-1} - V_n^- r^{-k_p-1}\right)\cos(k_p\theta+\omega t) - \sum_{k_m=1p,7p,\ldots}^{\infty} k_m\left(V_n^+ r^{k_m-1} - V_n^- r^{-k_m-1}\right)\cos(k_m\theta-\omega t) \tag{13}$$

B. Computation of the Flux Density in the Stator Core due to the Magnets

The aim of this subsection is to evaluate the magnetic field component in the stator core due to rotor magnets solely. For this purpose, it is assumed that, considering all magnetization patterns under study (Fig. 1), the rotor permanent magnets are arranged into uniformly-magnetized blocks. In order to simplify the computations, a group of $2p$ magnet blocks displaced by π/p mechanical radians apart (Fig. 3) is considered. Regardless of the magnetization pattern, the magnetization vectors of magnet blocks displaced by π/p mechanical radians are shifted by $180°$.

For the sake of simplicity, a new angular coordinate φ measured from the axis of the first block of the group is introduced so that a generic point p, in the rotor reference frame (Fig. 3), will be identified with the couple of polar coordinates (r,φ). This angular coordinate can be expressed as a function of θ as follows:

$$\varphi = \theta - \Theta, \text{ where, } \Theta = \frac{\omega t}{p} + \gamma, \text{ so, } \varphi = \theta - \frac{\omega t}{p} - \gamma, \tag{14}$$

where ω is the stator electric pulsation and γ is the angular shift between the stator s-axis and the rotor d-axis (Fig. 2).

After the magnetic field computation for this "magnet group" the resultant flux density, for all the magnetization patterns, can be computed extending the result using a finite sum of elements.

In a similar way as already done in the previous section, the vector potential in the stator core due to a magnet block group only ($\mathbf{\Phi}$), can be expressed by the Laplace equation:

$$\nabla^2\mathbf{\Phi} = \frac{1}{r}\frac{\partial}{\partial}\left[r\frac{\partial\Phi_z}{\partial r}\right] + \frac{1}{r^2}\frac{\partial^2\Phi_z}{\partial\theta^2} = 0 \quad \text{for } R_2 \le r \le R_3 \tag{15}$$

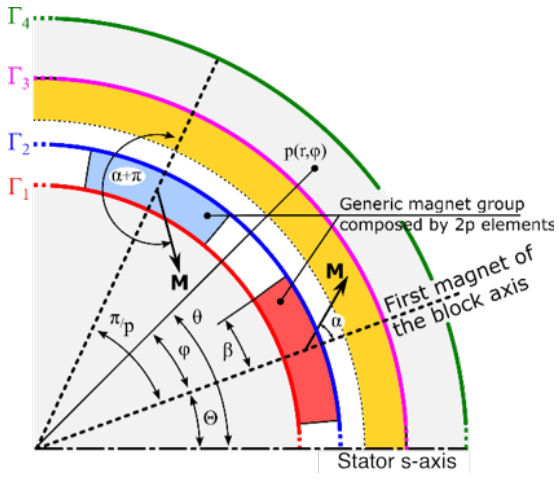

Fig. 3. Two magnet blocks displaced by one pole pitch. The set of $2p$ magnet blocks displaced by π/p mechanical radians around the rotor surface is referred to as a "group" of magnet blocks.

It is known that this kind of partial derivative differential equation has solutions that can be expressed also as follows:

$$\begin{aligned}&\Phi_z(r,\varphi,\alpha,\beta)=\\&\sum_{n=1,3,5,..}^{\infty}\left[G_n^+(\alpha,\beta)r^{np}+G_n^-(\alpha,\beta)r^{-np}\right]\sin(np\varphi)\\+&\sum_{n=1,3,5,..}^{\infty}\left[H_n^+(\alpha,\beta)r^{np}+H_n^-(\alpha,\beta)r^{-np}\right]\cos(np\varphi)\end{aligned}\tag{16}$$

Where the parameters $G_n^+(\alpha,\beta)$, $G_n^-(\alpha,\beta)$, $H_n^+(\alpha,\beta)$ and $H_n^-(\alpha,\beta)$ are function of the magnet block semi opening angle β and function of the magnetization vector orientation α. These parameters can be determined by imposing the following boundary conditions:

$$B_r^{rot}(R_3,\varphi,\alpha,\beta)=\frac{1}{R_3}\frac{\partial\Phi_z(R_3,\theta,\alpha,\beta)}{\partial\varphi}=0\tag{17}$$

along Γ_4 in Fig. 3.

$$B_r^{rot}(R_2,\varphi,\alpha,\beta)=\frac{1}{R_2}\frac{\partial\Phi_z(R_2,\theta,\alpha,\beta)}{\partial\varphi}=BR_r^{b.c.}(\varphi,\alpha,\beta),\tag{18}$$

along Γ_3 in Fig. 3.

In the same way as the previous section, the condition (17) is due to the fact that we want to impose the nullity of the magnetic field radial component along the circumference Γ_4. The other condition reported in (18) represents the continuity of the magnetic field radial component along the circumference Γ_3. The $BR_r^{b.c.}(\theta,t)$ function can be expressed using the results obtained in [6] as follows:

$$\begin{aligned}&BR_r^{b.c.}(\varphi,\alpha,\beta)=\\&\sum_{n=1,3,5,..}^{\infty}\left[X_n^+(\alpha,\beta)r^{np}+X_n^-(\alpha,\beta)r^{-np}\right]\sin(np\varphi)\\-&\sum_{n=1,3,5,..}^{\infty}\left[Y_n^+(\alpha,\beta)r^{np}+Y_n^-(\alpha,\beta)r^{-np}\right]\sin(np\varphi)\end{aligned}\tag{19}$$

Where the coefficients $X_n^+(\alpha,\beta)$, $X_n^-(\alpha,\beta)$, $Y_n^+(\alpha,\beta)$ and $Y_n^-(\alpha,\beta)$ can be found in the paper [6] at formulas (91)-(101).

By substituting (16) into (17) and putting to zero the coefficients of $\sin(np\varphi)$ and $\cos(np\varphi)$, two linear equations are obtained in the variables $G_n^+(\alpha,\beta)$, $G_n^-(\alpha,\beta)$, $H_n^+(\alpha,\beta)$ and $H_n^-(\alpha,\beta)$. Substituting (16) and (19) into (18) and equalling the coefficients of $\sin(np\varphi)$ and $\cos(np\varphi)$ two more linear equations are obtained in the same variables. Now, by solving this linear system we can obtain the desired variables and express them as follows:

$$\begin{aligned}G_n^+(\alpha,\beta)&=\frac{R_2^{2np}\cdot X_n^+(\alpha,\beta)+X_n^-(\alpha,\beta)}{R_2^{2np}-R_3^{2np}}\\G_n^-(\alpha,\beta)&=\frac{R_3^{2np}\left(R_2^{2np}\cdot X_n^+(\alpha,\beta)+X_n^-(\alpha,\beta)\right)}{R_3^{2np}-R_2^{2np}}\\H_n^+(\alpha,\beta)&=\frac{R_2^{2np}\cdot Y_n^+(\alpha,\beta)+Y_n^-(\alpha,\beta)}{R_2^{2np}-R_3^{2np}}\\H_n^-(\alpha,\beta)&=\frac{R_3^{2np}\left(R_2^{2np}\cdot Y_n^+(\alpha,\beta)+Y_n^-(\alpha,\beta)\right)}{R_3^{2np}-R_2^{2np}}\end{aligned}\tag{20}$$

The relationship between the magnetic vector potential and the flux density vector allows to derive the final expression for the magnetic radial and tangential components of the field in the stator core due to only a group of $2p$ magnets:

$$\begin{aligned}&B_r^{rot}(r,\theta,t,\alpha,\beta,\gamma)=\\&\sum_{n=1,3,5,..}^{\infty}\left[G_n^+(\alpha,\beta)r^{np-1}+G_n^-(\alpha,\beta)r^{-np-1}\right]\cdot\\&\cos(np\theta-n\omega t-np\gamma)\\-&\sum_{n=1,3,5,..}^{\infty}\left[H_n^+(\alpha,\beta)r^{np-1}+H_n^-(\alpha,\beta)r^{-np-1}\right]\cdot\\&\sin(np\theta-n\omega t-np\gamma)\end{aligned}\tag{21}$$

$$\begin{aligned}&B_\theta^{rot}(r,\theta,t,\alpha,\beta,\gamma)=\\&\sum_{n=1,3,5,..}^{\infty}\left[G_n^+(\alpha,\beta)r^{np-1}+G_n^-(\alpha,\beta)r^{-np-1}\right]\cdot\\&\sin(np\theta-n\omega t-np\gamma)\\-&\sum_{n=1,3,5,..}^{\infty}\left[H_n^+(\alpha,\beta)r^{np-1}+H_n^-(\alpha,\beta)r^{-np-1}\right]\cdot\\&\cos(np\theta-n\omega t-np\gamma)\end{aligned}\tag{22}$$

where φ is substituted using formula (14).

C. Computation of the Stator Core Total Magnetic Field for Every Rotor Magnetization Pattern

The evaluation of the total magnetic field distribution in the stator iron core is possible by superimposing the stator current contribution with the rotor magnet contribution. As already said in the first part of the paper, three different rotor magnetization patterns are considered for the total flux density evaluation. For this purpose, it is worth to notice that each magnetization pattern differs from the other only regarding the rotor contribution in the total magnetic field. The magnetic field component in the stator resultant from to the stator currents is the same for each case of magnetization. This said, it is possible to write the total magnetic field for the SPM slotless machine with a parallel magnetization as follows (Fig. 1a):

$$B_r^{par}(r,\theta,t,\gamma)=B_r^{st}(r,\theta,t)+B_r^{rot}(r,\theta,t,\bar{\alpha},\beta_{par},\gamma)\tag{23}$$

$$B_\theta^{par}(r,\theta,t,\gamma) = B_\theta^{st}(r,\theta,t) + B_\theta^{rot}(r,\theta,t,\bar{\alpha},\beta_{par},\gamma) \quad (24)$$

where

$$\beta_{par} = S_m \frac{\pi}{2p} \text{and } \bar{\alpha} = 0 \quad (25)$$

Equation (25) means that, in a parallel magnetized rotor, each pole is composed by only one parallel magnetized block so there is no sum to perform. The magnet block magnetization direction is the same as the block symmetry axis. S_m is the permanent magnet span over the pole pitch ratio.

Regarding the machine with the radial segmented SPM rotor (Fig. 1b), the total flux density distribution in the stator core domain can be expressed as follows:

$$B_r^{seg}(r,\theta,t,\gamma) = B_r^{st}(r,\theta,t) + \sum_0^{N_{seg}-1} B_r^{rot}\left[r,\theta-\tau_{seg}(2b+1),t,\bar{\alpha},\beta_{seg},\gamma\right] \quad (26)$$

$$B_\theta^{seg}(r,\theta,t,\gamma) = B_\theta^{st}(r,\theta,t) + \sum_0^{N_{seg}-1} B_\theta^{rot}\left[r,\theta-\tau_{seg}(2b+1),t,\bar{\alpha},\beta_{seg},\gamma\right] \quad (27)$$

where N_{seg} is the number of blocks composing a pole,

$$\tau_{seg} = S_m \frac{\pi}{2p} \text{ and } \beta_{seg} = S_m \frac{\pi}{2pN_{seg}} \quad (28)$$

According to equations (26) and (27), it is clear that a pole of the radial segmented rotor is composed by N_{seg} parallel magnetized blocks each with the magnetization direction correspondent to the block symmetry axis ($\bar{\alpha} = 0$).

In the end, for the machine with the halbach array SPM rotor (Fig. 1c), the total flux density distribution in the stator core domain can be presented as:

$$B_r^{hal}(r,\theta,t,\gamma) = B_r^{st}(r,\theta,t) + \sum_0^{N_{seg}-1} B_r^{rot}\left[r,\theta-\tau_{hal}(2b+1),t,\bar{\alpha(b)},\beta_{hal},\gamma\right] \quad (29)$$

$$B_\theta^{hal}(r,\theta,t,\gamma) = B_\theta^{st}(r,\theta,t) + \sum_0^{N_{seg}-1} B_\theta^{rot}\left[r,\theta-\tau_{hal}(2b+1),t,\bar{\alpha(b)},\beta_{hal},\gamma\right] \quad (30)$$

where N_{seg} again is the number of blocks per pole and:

$$\tau_{hal} = S_m \frac{\pi}{2p} \text{ and } \beta_{hal} = S_m \frac{\pi}{2pN_{seg}} \quad (31)$$

The direction of the magnetization vector for each block with respect to its symmetry axis is written as:

$$\bar{\alpha(b)} = p\left[\beta_{hal}(2b+1)\right] \quad (32)$$

D. Considerations on the Stator Core Magnetic Field

In some core loss evaluation methods [13]–[15], it is necessary to derive the trajectory described by the flux density fundamental harmonic vector in any point of the iron core. In general, such trajectory is an ellipse (as already shown in [11]). Indeed, the availability of an analytical expression for the radial and tangential flux density distributions in the stator core allows the instantaneous computation of the ellipse trajectory of the magnetic field at any point of the stator core unlike finite element analysis. In Figure 4C the trajectory is shown for the flux density vector in points P_1 and P_2 for every machine architecture taken into account. All the derived equations underline the fact that the shape of the ellipse is strongly dependent only on the radial coordinate.

IV. Finite Element Validations

The final formulas for the flux density in the iron core are assessed by comparison with finite element results obtained on two different machines which main data are reported in Table I. The validation is performed considering each machine equipped with the different magnetisation patterns previously dealt with.

TABLE I
SPM Machine Data used for Finite Element Validations

Parameter	Machine specification	
	Machine 1	***Machine 2***
R_i	47.5 mm	47.5 mm
R_m	57.5 mm	57.5 mm
R_1	58.5 mm	58.5 mm
R_2	62.0 mm	62.0 mm
R_3	90.0 mm	90.0 mm
H_c	850 kA/m	850 kA/m
μ_{mag}	1	1
S_m	0.95	0.95
p	2	3

The comparison is made between the flux density computed analytically and with FEA along two different circumferences Γ_1 and Γ_2 as shown in Fig. 5A and B. In the same figure is also represented the flux density trajectory in two different stator core points P_1 and P_2 (Fig. 5C). Assuming that the major contribution of the field in the stator core comes from the fundamental component, it is possible to present the fundamental vector trajectory of the flux density by means of analytical formulas derived from (23) to (32) in Cartesian coordinate system (considering n and k_m equal to 1 and excluding the part of the solutions (12) and (13) with the coefficient k_p). The fundamental field vector describes an elliptical trajectory as predicted which is illustrated with the dashed line in Figs 4 and 5. It is noticeable that, for all the magnetisation arrangements considered, the deeper is the studied contour in the stator core, the lower is the magnitude of the radial component of the flux density and the more dominant the tangential component gets. A further emerging observation is that for the parallel and radial magnetisation cases, the elliptical trajectory described by the total field

vector (continuous red line) has a larger major diameter than the one corresponding to the fundamental field vector (dashed red line). However for the halbach magnetisation arrangement, both of the trajectories are almost coinciding. This validate the fact that the magnets with parallel and radial magnetisation generate a field that containing a larger harmonic contents with respect the the hallbach magnetisation case which produces an almost sinusoidal field's waveform. In the end, it is proved that the proposed method is in a very good agreement with the results derived from FEA for both machine polarities taken into account.

V. Conclusion

In this paper, an analytical solution of the magnetic flux density in the stator core of a slotless permanent magnet machine is derived taking into account both the armature reaction and the permanent magnet contribution. The resultant solution was adapted to be applicable to different SPM rotor magnetization patterns commonly used in synchronous machines. Results have been compared with finite element calculations showing very good accordance. Besides the straightforwardness and instantaneous estimation of the stator core field of slotless SPM machines, the formulations being presented could be directly used for the analytical computation of the core losses, including the eddy-current, hysteresis and other loss components. Further works will take this path in order to fully demonstrate the feasibility of this application and compare the estimated iron core losses with experimental measurements.

References

[1] A. Tessarolo, F. Luise, P. Raffin, and V. Venuti, "Multi-objective design optimization of a surface permanent-magnet slotless alternator for small power wind generation," in *Proc. Int. Conf. Clean Electr. Power (ICCEP)*, June 2011, pp. 371–376.

[2] F. Luise, A. Tessarolo, F. Agnolet, S. Pieri, M. Scalabrin, M. Di Chiara, and M. De Martin, "Design optimization and testing of high-performance motors: Evaluating a compromise between quality design development and production costs of a halbach-array pm slotless motor," *IEEE Ind. Appl. Mag.*, vol. 22, no. 6, pp. 19–32, Nov 2016.

[3] S. Jumayev, K. O. Boynov, J. J. H. Paulides, E. A. Lomonova, and J. Pyrhönen, "Slotless pm machines with skewed winding shapes: 3-d electromagnetic semianalytical model," *IEEE Transactions on Magnetics*, vol. 52, no. 11, pp. 1–12, 2016.

[4] N. Bianchi, S. Bolognani, and F. Luise, "Analysis and design of a pm brushless motor for high-speed operations," *IEEE Transactions on Energy Conversion*, vol. 20, no. 3, pp. 629–637, 2005.

[5] Z. Q. Zhu and D. Howe, "Instantaneous magnetic field distribution in permanent magnet brushless dc motors. iv. magnetic field on load," *IEEE Trans. Magn.*, vol. 29, no. 1, pp. 152–158, Jan 1993.

[6] A. Tessarolo, M. Bortolozzi, and C. Bruzzese, "Explicit torque and back emf expressions for slotless surface permanent magnet machines with different magnetization patterns," *IEEE Trans. Magn.*, vol. 52, no. 8, pp. 1–15, Aug 2016.

[7] P. Pfister and Y. Perriard, "Slotless permanent-magnet machines: General analytical magnetic field calculation," *IEEE Trans. Magn.*, vol. 47, no. 6, pp. 1739–1752, June 2011.

[8] K. Atallah, Zi Qiang Zhu, and D. Howe, "Armature reaction field and winding inductances of slotless permanent-magnet brushless machines," *IEEE Trans. Magn.*, vol. 34, no. 5, pp. 3737–3744, Sep. 1998.

[9] A. Rahideh, M. Mardaneh, and T. Korakianitis, "Analytical 2-d calculations of torque, inductance, and back-emf for brushless slotless machines with surface inset magnets," *IEEE Transactions on Magnetics*, vol. 49, no. 8, pp. 4873–4884, 2013.

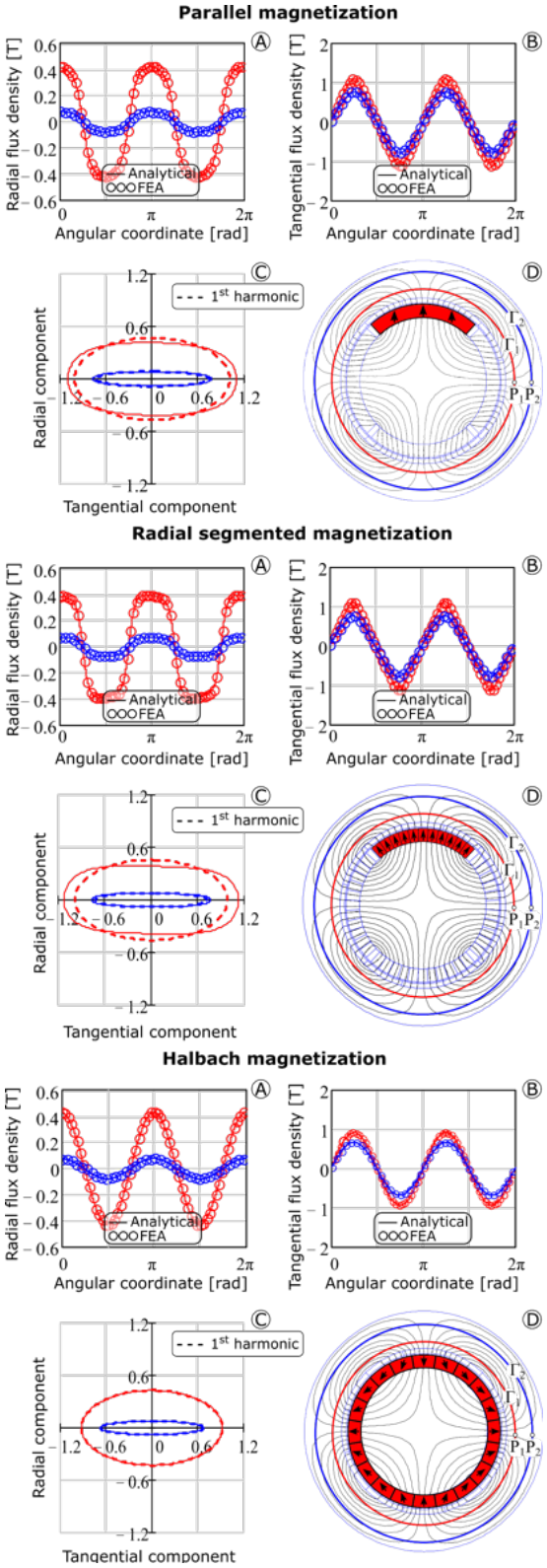

Fig. 4. **A** and **B**: comparison of the flux density components along the circumferences Γ_1 and Γ_2 for different rotor magnetization patterns; **C**: Flux density trajectory in P_1 and P_2; **D**: Machine under analysis cross section.

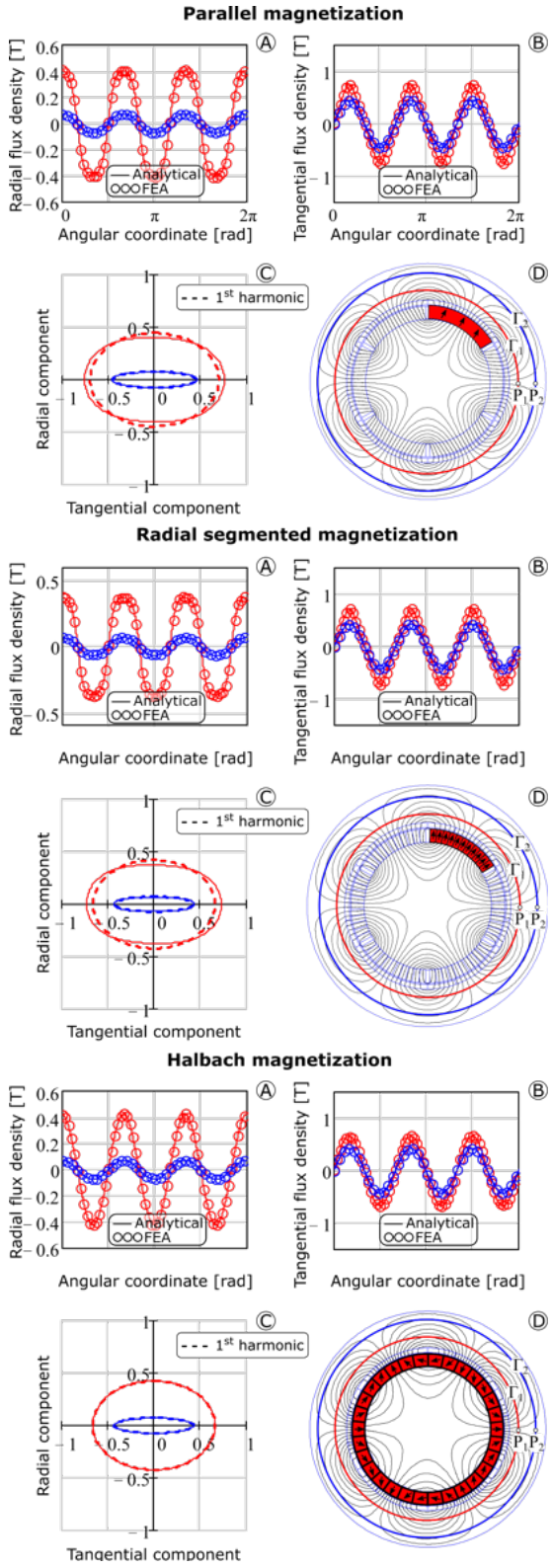

Fig. 5. **A** and **B**: comparison of the flux density components along the circumferences Γ_1 and Γ_2 for different rotor magnetization patterns; **C**: Flux density trajectory in P_1 and P_2; **D**: Machine under analysis cross section.

[10] A. Chebak, P. Viarouge, and J. Cros, "Analytical model for design of high-speed slotless brushless machines with smc stators," in *2007 IEEE International Electric Machines Drives Conference*, vol. 1, 2007, pp. 159–164.

[11] L. Branz, M. Bortolozzi, and A. Tessarolo, "Analytical calculation of the no-load flux density in the stator core of slotless spm machines," in *Proc. Int. Conf. Workshop Compatib. Power Electron.*, June 2013, pp. 244–249.

[12] G. Bertotti, "General properties of power losses in soft ferromagnetic materials," *IEEE Trans. Magn.*, vol. 24, no. 1, pp. 621–630, Jan 1988.

[13] K. Yamazaki and N. Fukushima, "Iron-loss modeling for rotating machines: Comparison between bertotti's three-term expression and 3-d eddy-current analysis," *IEEE Trans. Magn.*, vol. 46, no. 8, pp. 3121–3124, Aug 2010.

[14] J. V. Leite, M. V. Valência Ferreira da Luz, N. Sadowski, and P. A. da Silva, "Modelling dynamic losses under rotational magnetic flux," *IEEE Trans. Magn.*, vol. 48, no. 2, pp. 895–898, Feb 2012.

[15] C. A. Hernandez-Aramburo, T. C. Green, and A. C. Smith, "Estimating rotational iron losses in an induction machine," *IEEE Trans. Magn.*, vol. 39, no. 6, pp. 3527–3533, Nov 2003.

[16] P. H. Mellor and R. Wrobel, "Optimization of a multipolar permanent-magnet rotor comprising two arc segments per pole," *IEEE Trans. Ind. Appl.*, vol. 43, no. 4, pp. 942–951, July 2007.

[17] D. Lee, A. Jin, B. Min, L. Zheng, and K. Haran, "Optimisation method to maximise torque density of high-speed slotless permanent magnet synchronous machine in aerospace applications," *IET Elect. Power Appl.*, vol. 12, no. 8, pp. 1075–1081, 2018.

VI. Biographies

Nada Elloumi received the Engineering Diploma in Electro-mechanical Engineering and the M.Sc. degree in Sustainable Mobility Actuators: Research and Technology (SMART) from the National Engineering School of Sfax (ENIS), University of Sfax, Tunisia, in 2017. She is currently pursuing a joint Ph.D. in Electrical Engineering from the University of Sfax, Tunisia and the University of Trieste, Italy. Her main research activities focus on electric machine design, analysis and optimization for renewable energies and electric propulsion application.

Matteo Leandro (IEEE S'20) received the M.Sc. degree in electrical energy engineering from the University of Padova, Padua, Italy, in 2019. He is currently a PhD candidate at Department of Electric Power Engineering, Norwegian University of Science and Technology (NTNU), Trondheim, Norway. His current research interests include analytical formulations for electrical machine analysis, slotless machines and multiphysics. He is cooperating closely with Alva Industries AS, Trondheim, where his research is applied to analytical modeling and digital twin development of electric drives using slotless machines. The aim is to move towards development of lightweight coreless machines for aerial propulsion systems. Mr. Leandro regularly serves as a reviewer in several IEEE journals and conferences.

Jonas Kristiansen Nøland (IEEE S'14-M'17) received the Ph.D. degree in engineering physics from Uppsala University, Uppsala, Sweden, in 2017. He is currently an Associate Professor with the Department of Electric Power Engineering, Norwegian University of Science and Technology, Trondheim, Norway. His current research interests include excitation systems, large AC machines for aviation, magnetic levitation and electric transportation. Dr. Nøland is currently serving as an Editor for the IEEE TRANSACTIONS ON ENERGY CONVERSION.

Alberto Tessarolo received his Laurea and Ph.D. degrees in Electrical Engineering from the University of Trieste, Italy, and Padova, Italy, in 2000 and 2011, respectively. Before joining the University, he worked in the design and development of large innovative motors, generators and drives. Since 2006, he has been with the Engineering and Architecture Department of the University of Trieste, Italy, where he teaches the course of Electric Machine Design. He has authored over 150 international papers in the area of electrical machines and drives. He has been an associated editor for IEEE TRANS. ON ENERGY CONVERSION, IEEE TRANS. ON INDUSTRY APPLICATIONS and IET ELECTRIC POWER APPLICATIONS. He is the Editor-in Chief of the IEEE TRANS. ON ENERGY CONVERSION.